[5]D. R. Bates and R. McCarroll, Phil. Mag. Suppl. 11, 39 (1962).
[6]D. F. Gallaher and L. Wilets, Phys. Rev. 169, 139 (1968).
[7]I. M. Cheshire, D. F. Gallaher, and A. Joanna Taylor, J. Phys. B 3, 813 (1970).
[8]W. Lichten, Phys. Rev. 131, 229 (1963).
[9]W. Lichten, Phys. Rev. 139, A27 (1965).
[10]R. H. McKnight, Ph.D. thesis (University of Nebraska, 1970) (unpublished).
[11]W. R. Gibson, A. R. Johnston, R. J. Griffiths, and E. A. McClatchie, Nucl. Instr. Methods 33, 357 (1965).
[12]R. Avida and S. Gorni, Nucl. Instr. Methods 52, 125 (1967).
[13]S. J. Young, J. S. Murray, and J. R. Sheridan, Phys. Rev. 178, 40 (1969); also Dr. J. R. Sheridan (private communication).
[14]Joseph Macek and D. H. Jaecks, following paper, Phys. Rev. 4, 2288 (1971).
[15]D. H. Crandall and D. H. Jaecks, preceding paper, Phys. Rev. A 4, 2271 (1971).
[16]R. H. McKnight, D. H. Crandall, and D. H. Jaecks, Rev. Sci. Instr. 41, 1282 (1970).
[17]D. H. Crandall, R. H. McKnight, and D. H. Jaecks (unpublished); D. H. Jaecks, R. H. McKnight, and D. H. Crandall, Bull. Am. Phys. Soc. 15, 1503 (1970).
[18]L. T. Sin Fai Lam, Proc. Phys. Soc. (London) 92, 67 (1967).
[19]T. A. Green, Phys. Rev. 152, 18 (1966).
[20]R. K. Colegrave and D. B. L. Stephens, J. Phys. B 1, 428 (1968).
[21]R. McCarroll, R. D. Piacentini, and Salin, J. Phys. B 3, 1336 (1970).
[22]I. M. Cheshire, D. F. Gallaher, and A. J. Taylor, J. Phys. B 3, 813 (1970).

PHYSICAL REVIEW A VOLUME 4, NUMBER 6 DECEMBER 1971

Theory of Atomic Photon-Particle Coincidence Measurements*

Joseph Macek and D. H. Jaecks
Behlen Laboratory of Physics, The University of Nebraska, Lincoln, Nebraska 68508
(Received 18 March 1971)

The theory of measurements in which photons are detected in delayed coincidence with a scattered particle is developed in a form specifically applicable to atomic collisions. Equations are obtained which relate the measured coincidence rate to excitation amplitudes. These equations incorporate the polarization of the radiation, the fine and hyperfine structure of the atomic levels, the coherence of the radiation, and the time dependence of the radiation intensity. A semiclassical model for certain transitions is introduced to illustrate new features of coincidence measurements. The Ly-α transitions in hydrogen and $^1P \rightarrow {}^1S$ transitions in He are treated in detail to illustrate the general theory.

I. INTRODUCTION

Recently, coincidence techniques have been used to measure the amplitudes that describe atomic scattering processes. Three different types of measurements, distinguished by the types of particles detected, have been employed. Erhardt[1] has detected scattered electrons in coincidence with secondary electrons ejected in an ionizing collision of electrons with atomic helium. This represents a particle-particle coincidence measurement, and the data from such experiments can be directly interpreted in terms of differential ionization cross sections. Sheridan[2] has proposed measurements of photons emitted in the $D \rightarrow P$ transition of He in coincidence with a photon emitted in the subsequent $P \rightarrow S$ decay. This constitutes a photon-photon coincidence measurement, and the data can be interpreted in terms of the probabilities for these radiative transitions.[3] Jaecks *et al.*[4] have measured Ly-α photons emitted in the decay of the $2p$ states of hydrogen atoms formed by the charge exchange reaction

$$H^+ + A \rightarrow H^* + A^+$$

where A represents any target atom. This represents a photon-particle coincidence measurement, and, although similar experiments have been employed in nuclear physics, a theory relating experimental data to scattering amplitudes has not been given in a form directly applicable to atomic collisions. The theory[5] developed for nuclear studies is not directly applicable to atomic studies since nuclear studies have concentrated on determinations of the multipolarity of the electromagnetic transitions. In experiments of interest in atomic collision studies, the multipolarity of the radiative transitions is known, and experiments are conducted to determine the parameters of the population of states produced by the collision.

Recently, the theory of photon-particle coincidences has been developed in a form directly applicable to elementary particle reactions.[6] This theory emphasizes the determination of scattering amplitudes (or density matrix elements) from experimental data, and is more directly applicable

to atomic studies than is the theory developed for nuclear studies. Even this theory is not directly applicable, however, since the "beating" of radiation from different fine- and hyperfine-structure levels introduces oscillatory terms[7] in the radiative decay of excited atoms, whereas the theory of Ref. 5 assumes a purely exponential decay. In this paper we develop the theory of photon-particle coincidence in a form directly applicable to atomic collisions, taking into account the fine and hyperfine structure of atomic levels.

The first consistent treatment relating the number of photons emitted after an atomic collision to excitation cross sections was given by Percival and Seaton.[8] They did not consider the detection of scattered particles and photons in coincidence and therefore used a time independent theory with the further condition of incoherent excitation of magnetic substates. Since we are interested in coincidence experiments, and since modern electronics with resolution times of the order of nanoseconds are used in such experiments, it is necessary to consider the time dependence of the radiation. Furthermore the incoming particle beam and the axis of the particle detector define a plane, which we shall call the scattering plane, so that the geometry possesses only reflection symmetry in this plane rather than rotational symmetry about the beam axis. As a consequence of this lower symmetry the magnetic substates are coherently excited and interference between amplitudes referring to different magnetic sublevels occurs. The consequences of this interference is the subject of the study reported in Ref. 6. Although we develop the present theory from first principles without drawing on the theory previously developed to treat elementary particle decays, our final results essentially combine the existing theories of angular correlations and time resolved spectroscopy to obtain expressions for the number of coincidences in a form directly applicable to atomic collisions. This theory is presented in Sec. II. The theory relates the number of coincidences measured for a given orientation of photon and particle detectors to the amplitudes describing the formation of the decaying states. The amplitudes are treated as parameters to be fitted to the experimental data. The atomic level structure and the radiative decay widths are assumed known, although they may also be treated as fitting parameters.

Section IV treats the time dependence in more detail than is given in Sec. II. Earlier treatments[9] of the time dependence of the radiation in cross section measurements considered the time development of the number of atoms in excited states by means of rate equations, and then supposed that the number of photons observed was proportional to the number of excited atoms at each instant of time. This supposition is rigorously correct only when the number of photons integrated over all angles of emission and summed over all polarizations is measured. Most experiments detect light emitted in a definite direction and polarization corrections are needed to relate the measured intensity to the number of excited atoms. It has been shown that the polarization is time dependent,[7] and this time dependence has not been considered in earlier theories. Section IV treats the time dependence in detail and defines conditions under which a rate equation approach applies.

The discussion in Sec. II is quite general and the theory presented there applies to a wide variety of collisional processes. The development is necessarily mathematical and somewhat abstract; consequently it is difficult to relate the final equations to a simple physical picture of the production of line radiation excited by atomic collisions. Under certain conditions the angular distribution of light can be described in terms of a simple classical source and this source related directly to the collisional process. This construction provides a ready picture of the otherwise obtuse results of Sec. II and is discussed in Sec. III.

Although our theory has as its main objective the development of expressions for photon-particle coincidences, it also applies to noncoincidence experiments which measure cross sections by optical techniques. In particular, the theory extends the treatment of Percival and Seaton[8] to include expressions for the polarization of radiation emitted in charge-exchange collisions. We find that as long as *LS* coupling holds and as long as the emitting atom remains in view of the photon detector for a time long compared to the mean life, Percival and Seaton's expressions apply. The appropriate modifications when one or the other of these assumptions fails are discussed in Secs. II and IV.

II. GENERAL THEORY OF PHOTON-PARTICLE COINCIDENCES

A. *LS* Coupling

The general theory of photon-particle coincidences proceeds most rigorously from the quantum theory of radiation.[3] The alternative approach of Franken,[10] however, provides a more simple but entirely adequate point of departure, which we will follow here. This theory assumes that cascade contributions are negligible, and that the light detection system detects all radiation with a frequency near the central frequency of a fine-structure or hyperfine-structure multiplet. The sensitive frequency range is assumed to be sufficiently broad that little intensity is contained in the undetected wings of the emission lines. These same assump-

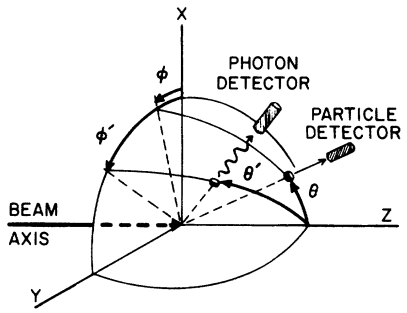

FIG. 1. Schematic collision geometry. Primed and unprimed coordinates indicate the photon detector and particle detector positions.

tions are involved in Ref. 3; indeed the deviation in this section follows the earlier discussion very closely except that cylindrical symmetry is not assumed. However, the formulas of Ref. 3 can be recovered from those derived here by integrating Eq. (21) of this paper over the azimuthal directions of the detected particle. This integration implies cylindrical symmetry, and therefore some of the results we obtain here, for example, expressions for the sum of Clebsch-Gordan coefficients, can be applied to the analysis of atomic lifetime measurements using beam-foil techniques.

We consider a collision in which a molecule, ion, or electron strikes an atom or molecule. In the collision some excited atoms are produced which subsequently decay by photon emission. The experiment measures the number of these photons in coincidence with some scattered particle, which may be an electron, atom, or molecule. We seek an expression relating the coincidence rate dN_c to the amplitudes describing the excitation process. We stress here that the collision may involve molecules of any complexity, but the photons must come from an atom. We suppose that the atomic levels are adequately described by LS coupling.

The coincidence rate depends upon the position of the photon and particle detectors. A schematic experimental arrangement with an associated coordinate system is shown in Fig. 1. The incoming beam axis is taken to be the z axis, and the x-z plane is located arbitrarily. The angular coordinates of the particle detector relative to this coordinate system are denoted by θ and ϕ, and the coordinates of the photon detector by θ' and ϕ'. We seek an expression for dN_c in terms of these four angles. In all practical cases the collision takes place in a time that is short compared to the radiative lifetime. Thus the wave function for the excited atom at $t=0$ is

$$|\psi) = \sum_{JFM_F} a(JFM_F)\,|JFM_F)\,, \tag{1}$$

where $|JFM_F)$ is the state vector describing a particular atomic state with total angular momentum F and electron angular momentum J, and $a(JFM_F)$ is the amplitude for producing the excited state. Because $a(JFM_F)$ is a scattering amplitude, it depends upon θ and ϕ, the coordinates of the particle detector. The state vector (1) is not an eigenstate of the Hamiltonian. Consequently at a later time the atom is in the state

$$|\psi) = \sum_{JFM_F} a(JFM_F)\,|JFM_F) e^{-(\gamma/2+iE_{JF}/\hbar)t}\,, \tag{2}$$

where the factor $e^{-\gamma t/2}$ is included to account for the decay of the upper level population. Here $1/\gamma$ is the mean life of the excited atom. Note that the time is measured from the instant of collision.

The coincidence rate is proportional to the square of the dipole matrix element describing the decay integrated over the resolution time of the circuits

$$dN_C = v n_0 n_A (e^2\omega^3/2\pi hc^3) \sum_0 \int_0^{\Delta t} dt\,|\,(0\,|\,\hat{\epsilon}\cdot\vec{\mathbf{X}}\,|\,\psi)\,|^2\,, \tag{3}$$

where n_0 is the density of particles in the incoming beam, v is the velocity of the beam, n_A is the number of target atoms in the scattering volume, ω is the frequency of the emitted light, Δt is the resolution time of the circuits, $\hat{\epsilon}$ is the polarization vector of the detected light, and $(0|$ is the state vector for the lower levels reached in the decay. The quantum numbers of the lower levels are summed over after squaring the matrix element. In Eq. (3) we have supposed that all photons emitted in a definite direction in the time interval $0-\Delta t$ are detected. In Read's[11] application of coincidence techniques to lifetime measurements, photons emitted at a much later time are detected. Then the limits of the time integration are t_i and $t_i+\Delta t_i$, where t_i is the delay time beyond that required for the transit of the scattered particle to the detector. In Sec. IV we will consider specific experimental geometries with t_i unequal to zero. The polarization vector $\hat{\epsilon}$ is determined by the geometry of the photon detection system, and depends upon the coordinates θ' and ϕ' of the photon detector. Since the amplitudes $a(JFM_F)$ have dimensions of length the quantity $dN_c/d\Omega\,d\Omega'$ is seen to be a rate equal to the number of counts per unit of time.

Writing $\hat{\epsilon}$ in terms of its spherical components, substituting Eq. (2) into Eq. (3) and denoting the angular momentum quantum numbers of the lower levels explicitly, we find for $dN_c/d\Omega\,d\Omega'$

$$\frac{dN_c}{d\Omega\,d\Omega'} = v n_0 n_A (e^2\omega^3/2\pi hc^3) \times \sum_{qq' JFM_F J'F'M'_F M_{L_0} M_{S_0} M_{I_0}} a^*(J'F'M'_F)\,a(JFM_F)$$

$$\times(-)^{q+q'}\epsilon^{*}_{-q'}\epsilon_{-q}$$

$$\times(L_0M_{L_0}S_0M_{S_0}I_0M_{I_0}\,|\,X'_q\,|\,LS(J')IF'M'_F)^{*}$$

$$\times(L_0M_{L_0}S_0M_{S_0}I_0M_{I_0}\,|\,X_q\,|\,LS(J)IFM_F)$$

$$\times\int_0^{\Delta t}dt\,e^{-(\gamma+i\omega_{JFJ'F'})t}\,, \qquad (4)$$

where

$$\omega_{JFJF'}=(E_{JF}-E_{J'F'})/\hbar.$$

Equation (4) is just Eq. (1.2) of Ref. 10 integrated over the resolution time.

Let us consider Eq. (4) in some detail. Basically it contains three different types of terms: (a) the scattering amplitudes describing the excitation process, (b) the dipole matrix elements describing the decay, and (c) the time-dependent factor. The scattering amplitudes are here considered as unknown parameters to be fitted to the experimental data. Because the amplitudes describe the scattering, they are functions of θ and ϕ, the coordinates of the particle detector. Later we will use the transformation properties of the amplitudes under rotations about the incoming beam axis to consider unknown parameters which are functions of θ only.

The dipole matrix elements and the polarization vectors constitute the second type of term. They describe the radiative decay of the upper levels. The polarization vectors are determined by the geometrical arrangement of the photon detection system, and are therefore known completely. The value of the dipole transition matrix element is assumed known from theory or from other experimental data. It can also be treated as a fitting parameter, however.

The third term describes the time dependence of the emitted light. Note that in addition to the usual exponential factor $e^{-\gamma t}$, it contains an oscillatory factor $e^{i\Omega t}$, where we have used Ω to denote any one of the frequencies $\omega_{JFJ'F'}$. This oscillatory factor describes the modulation of the light intensity due to interference of radiation from the coherently excited levels of the fine-structure or hyperfine-structure multiplet. Effects of this term have been observed in radiation from atoms excited by beam-foil collisions.[11,12] Percival and Seaton's[8] theory also contains this particular term, but with Δt taken equal to infinity. This is appropriate for experiments in which all light emitted in the particular transition under study is collected regardless of the time of emission. It is not appropriate for a coincidence experiment, or for a charge-exchange experiment where the emitting atom may be viewed for a time short compared to the decay time.

Equation (4) is the basic equation of our theory. However, it is not yet in a form suitable for application. In line with our supposition that LS coupling holds, we may reduce the number of independent parameters by expressing the amplitude and the state vectors in the LM_L representation. The state vectors $|\,LS(J)IFM_F)$ are written in terms of the state vectors $|\,LM_L\,SM_SIM_I)$ according to the usual vector coupling rules

$$|\,LS(J)IFM_F)=\sum_{M_L\,M_S\,M_I\,M_J}|\,LM_LSM_SI\,M_I)$$

$$\times(LM_LSM_S\,|\,LSJM_J)(JM_JIM_I\,|\,JIFM_F)\,. \qquad (5)$$

Similarly, we have

$$a(JFM_F)=\sum_{\bar{M}_L\bar{M}_S M_I M_J}a(L\bar{M}_LS\bar{M}_SIM_I)$$

$$\times(L\bar{M}_LS\bar{M}_S\,|\,LSJM_J)(JM_JIM_I\,|\,JIFM_F)\,. \qquad (6)$$

The amplitudes $a(LM_LSM_SIM_I)$ occur in Eq. (4) as products

$$a^{*}(LM'_LSM'_SIM'_I)\,a(LM_LSM_SIM_I)\,. \qquad (7)$$

To obtain the number of photons counted in a unit time interval, Eq. (4) and hence also Eq. (7) is averaged over initial states and summed over final states. We denote this sum and average by S. To evaluate this sum we now express the amplitudes explicitly as the matrix elements of transition operators,

$$a(LM_LSM_SIM_I)=(i\vec{k}_i\,|\,T\,|\,\vec{k}_f\vec{K}_1\vec{K}_2\cdots f,\,LM_LSM_SIM_I),$$

where i is the set of quantum numbers describing the internal state of both particles before collision, $\vec{k}_i$ is the momentum vector of the incoming particle, $\vec{k}_f$ is the momentum vector of the outgoing particle detected by the particle detector, the $\vec{K}_i$'s are the momentum vectors of all particles not detected by the particle detector, f represents the set of all quantum numbers describing the internal state of all particles except the radiating atom, and $LM_LSM_SIM_I$ refer to the excited states of the atom emitting the detected radiation. The sum denoted by S then corresponds to an average over i, a sum over f, and an integration over all momentum vectors $\vec{K}_i$ of the undetected particles

$$S\,a^{*}(LM'_LSM'_SIM'_I)a(LM_LSM_SIM_I)$$

$$=\frac{1}{W_i}\sum_i\sum_f\int\prod_r d\hat{K}_r$$

$$\times(i\vec{k}_i\,|\,T\,|\,\vec{k}_f\vec{K}_1\vec{K}_2\cdots f,\,LM'_LSM'_SIM'_I)$$

$$\times(i,\vec{k}_i\,|\,T\,|\,\vec{k}_f\vec{K}_1\vec{K}_2\cdots f,\,LM_LSM_SIM_I)\,, \qquad (8)$$

where W_i is the statistical weight of the initial state.

Several details in this expression should be

noted. First, notice that both T-matrix elements refer to the same final state of all particles except the emitting atom. The initial states are the same since the wave function, Eq. (1), refers to the state formed in a particular collision, i.e., a collision in which the initial state is specified by a definite set of quantum numbers i. The final states of the nonemitting particles, whose quantum numbers are denoted by f, could in general be different in the two matrix elements; however, the condition that the collision time is much shorter than the lifetime of the decaying states implies that any change of state of the nonemitting particles cannot affect the radiative decay of the atom whose radiation is detected. Thus the f quantum numbers are also the same. Further, since the z projection of the total electronic spin is conserved in the collision, and since both matrix elements contain the same i and f quantum numbers, we must have

$$M_S = M_{S'} \ . \tag{9}$$

Similarly we have

$$M_I = M_{I'} \ . \tag{10}$$

To factor out the ϕ dependence of the product of amplitudes, we consider the transformation of this product under two different rotations: (a) any rotation of the arbitrary coordinate variables $\vec{r}_s$ integrated over in forming the T-matrix elements, and (b) a rotation of the directions of all outgoing particles about the beam axis. The first transformation cannot affect the value of the matrix element, but the second rotation does since it describes a new physical arrangement. The effect of the second rotation is the same as the effect of the combined rotations (a) and (b). Under these simultaneous rotations the plane-wave factors $|\vec{k}_f)$ and $|\vec{K}_i)$ do not change since they are functions of the dot product $\vec{K}_s \cdot \vec{r}_s$ only. The states labeled by the internal quantum numbers i, f, M_L, M_S, and M_I transform as

$$\begin{aligned} &|i) \to e^{iM_i\phi}\,|i) \ , \\ &|f,\ M_L M_S M_I) \to e^{i(M_f+M_L+M_S+M_I)\phi}\,|f,\ M_L M_S M_I) \ . \end{aligned} \tag{11}$$

These transformation equations and Eqs. (9) and (10) imply that

$$S a^*(M_L', M_S' M_I')\, a(M_L M_S M_I)$$

TABLE I. Spherical-tensor components of the two polarization vectors $\hat{\epsilon}^{(1)}$ and $\hat{\epsilon}^{(2)}$.

$q=$	1	0	-1
$\hat{\epsilon}^{(1)}$	$-\cos\theta'\, e^{i\phi'}/\sqrt{2}$	$-\sin\theta'$	$\cos\theta'\, e^{-i\phi'}/\sqrt{2}$
$\hat{\epsilon}^{(2)}$	$-i\, e^{i\phi'}/\sqrt{2}$	0	$-i\, e^{-i\phi'}/\sqrt{2}$

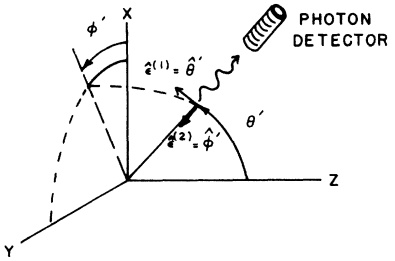

FIG. 2. Standard polarization vectors $\hat{\epsilon}^{(1)}$ and $\hat{\epsilon}^{(2)}$.

$$= \delta_{M_S' M_S}\, \delta_{M_I' M_I} \langle a_{M_L'}\, a_{M_L} \rangle\, e^{i(M_L - M_L')\phi}/(2S+1)\,(2I+1) \ , \tag{12}$$

where we have used brackets to denote the average previously denoted by S, and where we have introduced amplitudes a_{M_L}. These amplitudes differ from the amplitudes $a(LM_L SM_S IM_I)$ in that a_{M_L} is normalized so that $|\, a_{M_L}\,|^2$ is equal to the partial cross section for exciting the M_Lth magnetic substate of the decaying states, and a_{M_L} is a function of θ only.

A similar consideration of the transformation properties of the amplitudes under reflections in the scattering plane shows that

$$\langle a_{M_L'}\, a_{M_L} \rangle = (-1)^{M_L - M_L'} \langle a_{-M_L'}\, a_{-M_L} \rangle \ . \tag{13}$$

Here and throughout this paper we are assuming the Condon-Shortley phase convention. Equations (12) and (13) enable the coincidence rate to be expressed in terms of a minimum number of parameters $\langle a_{M_L'}\, a_{M_L} \rangle$ which depend only upon the angular coordinate θ. The parameters are often denoted as density matrix elements $\rho_{M_L' M_L}$. However the present notation emphasizes their connection with the scattering amplitudes more commonly used in excitation studies.

Now consider the polarization vector $\hat{\epsilon}$. For every direction of the outgoing photon, only two polarization directions are linearly independent. It is convenient to express an arbitrary polarization vector $\hat{\epsilon}$ in terms of two independent unit vectors perpendicular to the detector axis. We choose (Fig. 2) one vector $\hat{\epsilon}^{(1)}$ lying in plane formed incoming beam and the photon detector axis and pointing in the direction of increasing θ'. The other vector $\hat{\epsilon}^{(2)}$ is perpendicular to both $\hat{\epsilon}^{(1)}$ and the photon detector axis, and points in direction of increasing ϕ'. The spherical components of these two vectors are given in Table I. An arbitrary polarization vector $\hat{\epsilon}$ oriented at an angle β with respect to $\hat{\epsilon}^{(1)}$ is then given by

$$\hat{\epsilon} = \hat{\epsilon}^{(1)} \cos\beta + \hat{\epsilon}^{(2)} \sin\beta \ . \tag{14}$$

Substituting Eqs. (5), (6), (12), (14), and the expressions for $\hat{\epsilon}^{(i)}$ from Table I into Eq. (4), and using the Wigner-Eckart theorem to evaluate the dipole matrix element, we obtain

$$dN_c = vn_0 n_A(3\gamma'/8\pi)\{A_{00}\cos^2\beta + A_{11}\sin^2\beta + (A_{11}-A_{00})\cos^2\beta\cos^2\theta'$$
$$+\sqrt{2}\,\mathrm{Re}A_{01}[\sin 2\theta'\cos^2\beta\cos(\phi-\phi') + \sin 2\beta\sin\theta'\sin(\phi-\phi')] - \mathrm{Re}A_{1-1}[(\cos^2\beta\cos^2\theta' - \sin^2\beta)$$
$$\times\cos 2(\phi-\phi') + \sin 2\beta\cos\theta'\sin 2(\phi-\phi')]\}\,d\Omega d\Omega' , \quad (15)$$

where

$$A_{qq'} = \sum_{JFJ'F'M_LM_L'} U(qq'M_LM_L'JFJ'F'LL_0)\langle a_{M_L'}\, a_{M_L}\rangle \int_0^{\Delta t} dt\exp[-(\gamma + i\omega_{JFJ'F'})t] , \quad (16)$$

with

$$U(qq'M_LM_L'JFJF'LL_0) = \sum_{M_FM_JM_F'M_J'\bar{M}_J\bar{M}_J'M_SM_IM_{L_0}M_{I_0}M_{S_0}\bar{M}_L\bar{M}_L'} (L\bar{M}_LSM_{S_0}\,|\,LSJM_J)(JM_JIM_{I_0}\,|\,JIFM_F)$$
$$\times(L_0M_{L_0}1q\,|\,L_01L\bar{M}_L)(L\bar{M}_L'SM_{S_0}\,|\,LSJ'M_J')(J'M_J'IM_{I_0}\,|\,J'IF'M_F')(L_0M_{L_0}1q'\,|\,L_01L\bar{M}_L')$$
$$\times(LM_LSM_S\,|\,LSJ\bar{M}_J)(J\bar{M}_JIM_I\,|\,JIFM_F)(LM_L'SM_S\,|\,LSJ'\bar{M}_J')(J'\bar{M}_J'IM_I\,|\,J'IF'M_F')[1/(2S+1)(2I+1)] , \quad (17)$$

and where

$$\gamma' = (8\pi/3)\,|\,(L\,\|X_q\|\,L_0)\,|^2/(2L+1) \quad (18)$$

is the partial decay width for producing the detected photon. In general γ' is not equal to the decay width γ, whose reciprocal is related to the mean life of the excited atom. The quantity γ' is given by the branching ratio B for the observed transition times γ,

$$\gamma' = B\gamma . \quad (19)$$

The sum which represents U in Eq. (17) can be simplified by standard techniques. The reduction of U to a simple form has been carried out in general in the Appendix. To evaluate the sum representing U we need only identify the quantum numbers in Eqs. (A1) and (A12) of the Appendix. Comparing Eq. (17) and Eq. (A1) we find that U is given by Eq. (A12) if we identify j_i, k_i, and l_i according to

$$j_6 = k_6 = j_2 = k_2 = L , \qquad k_4 = F' ,$$
$$l_2 = l_5 = S , \qquad j_4 = F ,$$
$$l_3 = l_4 = I , \qquad m_1 = q ,$$
$$k_3 = k_5 = J' , \qquad m_2 = M_L ,$$
$$k_1 = j_1 = 1 , \qquad r_1 = q' ,$$
$$k_6 = L_0 , \qquad r_2 = M_{L'} ,$$
$$j_3 = j_5 = J .$$

Then we find for U

$$U(qq'M_LM_L'JFJ'F'\ LL_0) = [(2J+1)(2J'+1)(2F+1)(2F'+1)(2L+1)/(2S+1)(2I+1)]\,(-)^{L_0+q-M_L}$$
$$\times\sum_{\chi\nu}(2\chi+1)(-)^{-\chi}\begin{Bmatrix} L & L & \chi \\ J' & J & S\end{Bmatrix}^2\begin{Bmatrix} J & J' & \chi \\ F' & F & I\end{Bmatrix}^2\begin{Bmatrix} L & L & \chi \\ 1 & 1 & L_0\end{Bmatrix}\begin{pmatrix} L & L & \chi \\ -M_L' & M_L & \nu\end{pmatrix}\begin{pmatrix} 1 & 1 & \chi \\ -q & q' & -\nu\end{pmatrix} . \quad (20)$$

Equation (20) is convenient for both the numerical evaluation of U and for the study of the symmetry properties of U under interchanges of the indices. The sum on the right-hand side can be easily evaluated numerically since χ takes on only the values 0, 1, and 2. Tables of the 3- and 6-j symbols when one of the arguments is 0, 1, or 2 are given by Edmunds.[13]

The symmetry properties of the U coefficients can be used to reduce the number of different terms. From the symmetry of the 6-j symbols it follows that U is invariant to the simultaneous interchange of q and q' and M_L and M_L'. Further, U is invariant to a simultaneous change of sign of q, q', M_L, and M_L'. We have already used these symmetry relations and Eq. (13) to obtain the expression in Eq. (15).

When no polarization measurement is performed the number of coincidences is proportional to dN_c of Eq. (15) summed over two independent polarizations. Summing Eq. (15) over two polarization directions, say β and $\beta + \frac{1}{2}\pi$, gives

$$dN_c = vn_0n_A\gamma'(3/8\pi)[A_{00} + A_{11} + (A_{11}-A_{00})\cos^2\theta'$$
$$+\sqrt{2}\,\mathrm{Re}A_{01}\sin 2\theta'\cos(\phi-\phi')$$

$$+A_{1-1}\sin^2\theta'\cos 2(\phi-\phi')]\,d\Omega d\Omega' \ . \qquad (21)$$

Equation (21) has been used previously by one of the authors to interpret data on the charge exchange of protons on helium.[4] When Eq. (21) is integrated over $d\phi$ or $d\phi'$ the last two terms average to zero, and Eq. (21) reduces to the results of Percival and Seaton provided Δt is taken to be infinite in Eq. (16).

Equations (15) and (21) apply to a wide variety of atomic processes. For all such processes, the information obtainable in a coincidence experiment may be expressed in terms of the four quantities A_{00}, A_{11}, $\mathrm{Re}A_{01}$, and A_{1-1}. The theory given above then relates these quantities to the density matrix elements $\langle a_{M_L'} a_{M_L}\rangle$ which describe the excitation process. Alternatively, the density matrix elements may be calculated theoretically and the quantities $A_{q'q}$ then calculated from Eq. (16). Theoretical calculations have usually been directed toward obtaining cross sections, or equivalently, the quantities A_{00} and A_{11}. In order to more thoroughly relate theory and experiment it is desirable to present the quantities A_{01} and A_{1-1} as well.

To give some indication of the significance of the quantities A_{01} and A_{1-1} we consider in this section, and in Sec. IV, two special cases which illustrate the general features of the angular distribution. We consider radiation from $P\to S$ transitions excited by an atomic collision where the initial states of both incoming particles are S states, and where there are only two particles in the final state with the nonradiating particle also in an S state. Then reflection symmetry in the plane of scattering implies that $a_1 = -a_{-1}$. Thus we have

$$\langle a_{-1}a_1\rangle = -|a_1|^2 = -\sigma_1 \qquad (22)$$

and the quantity A_{1-1} can be written in terms of the partial cross section for exciting the $M_L = \pm 1$ states.

1. $^1P \to {}^1S$ *Transitions in* He

We now consider the $^1P\to{}^1S$ transitions in He, excited by electron or proton impact, for example. This case is interesting because the ^1P states of He[4] have no fine or hyperfine structure, therefore the time-dependent exponential is just $e^{-\gamma t}$ and is common to all terms in Eq. (16). Also the lifetime of these excited states is short compared to experimentally realizable resolution times so we may take Δt to be infinite. Then using Eq. (22) in Eq. (16) we find

$$\begin{aligned} A_{00} &= \sigma_0/\gamma \ , \\ A_{11} &= -A_{1-1} = \sigma_1/\gamma \ , \\ A_{01} &= \mathrm{Re}\langle a_0 a_1\rangle/\gamma \ . \end{aligned} \qquad (23)$$

When the photon detector is placed so that it views photons emitted perpendicular to the scattering plane, then both θ' and $\phi-\phi'$ equal 90° and Eq. (21) becomes

$$dN_c = vn_0 n_A(\gamma'/\gamma)(3/8\pi)[\sigma_0+2\sigma_1]\,d\Omega d\Omega' \ . \qquad (24)$$

We see that the number of coincidences for this particular geometry is proportional to the cross section summed over magnetic substates. This result will be further discussed in Sec. IV.

2. Ly-α *Transition in* H

Because of the simplicity of the hydrogen atom, the study of atomic excitation processes involving it have always occupied an important position in the theoretical and experimental literature. Coincidence measurements of A_{01} and A_{1-1} will further our understanding of these excitation processes since the relative phase of a_0 and a_1 can be extracted if A_{00}, A_{11}, and A_{01} are known.

The Ly-α radiation is emitted from excited atoms in the $2p$ states. These states have both fine and hyperfine structure, consequently the time-dependent factor in Eq. (16) does not factor out as is the case for $^1P\to{}^1S$ transitions in He. Since the hyperfine structure of both the $^2P_{1/2}$ and the $^2P_{3/2}$ levels is small compared to their decay widths, we may set $\omega_{JFJ'F'}$ equal to zero to a good approximation. Further since the precession period $1/\omega_{JJ'}$ and the mean life $1/\gamma$ are much shorter than commonly employed resolution times, the time integral in Eq. (16) becomes approximately

$$\int_0^\infty dt\,\exp[-(\gamma+i\omega_{JJ'})t] = \frac{1}{\gamma+i\omega_{JJ'}} \approx \begin{cases} 0 \ , & J\neq J' \\ 1/\gamma \ , & J=J' \end{cases} \ . \qquad (25)$$

With these approximations we find

$$\begin{aligned} A_{00} &= (5\sigma_0+4\sigma_1)/9\gamma \ , \\ A_{11} &= (2\sigma_0+7\sigma_1)/9\gamma \ , \\ A_{01} &= \mathrm{Re}\langle a_0 a_1\rangle/3\gamma \ , \\ A_{1-1} &= -\sigma_1/3\gamma \ . \end{aligned} \qquad (26)$$

When the photon detector axis is perpendicular to the scattering plane, Eq. (21) becomes

$$dN_c = vn_0 n_A(3/8\pi)(7/9)[\sigma_0+2\sigma_1]\,d\Omega d\Omega' \ . \qquad (27)$$

This result is identical to Eq. (24) except for the factor of $\frac{7}{9}$. This factor represents a reduction in the number of photons emitted perpendicular to the scattering plane because the fine structure causes the angular distribution to smear out. This observation will be further developed in Sec. IV.

B. *LS* Coupling Violated in Collision

With a redefinition of $A_{qq'}$, Eqs. (15) and (21) also apply when *LS* coupling does not hold. Two somewhat different situations may occur here: (a) The radiating atom may violate *LS* coupling, or (b) some nonradiating atom taking part in the collision may violate *LS* coupling. We consider case (a) first.

1. *Radiating Atom Violating LS Coupling*

In this case the scattering amplitudes referring to states with different J values are no longer related by the transformation of Eq. (6), but are treated as independent fitting parameters. Similarly the level width is also a function of J. Now a particular experiment may resolve the light from levels of the same multiplet with different J quantum numbers. Therefore, we are interested in expressions analogous to Eq. (16), but with J no longer summed over. Even when the light from different J levels is not resolved, the breakdown of *LS* coupling implies that the splittings are large compared to the level widths. Then $\omega_{JJ'}$ in Eq. (16) is large compared to γ and the time-dependent factors for $J \neq J'$ are small compared to those with $J = J'$ and terms with $J \neq J'$ can be neglected, i.e., the radiation from different J levels adds incoherently. Then the contribution from all levels with different J values is just the sum of the individual contributions. Only interference of radiation from different hyperfine levels need be considered. The required expression for $A_{qq'}$ is then obtained by replacing L by J, J by F, J' by F', S by I, I by 0, L_0 by J_0, M_L by M_J, and $M_{L'}$ by $M_{J'}$ in Eqs. (16) and (20), with a corresponding identification for the primed quantum numbers. We then have for $A_{q'q'}$

$$A_{qq'} = \sum_{FF'M_JM'_J} U(qq' M_J M'_J FF' J J_0) \langle a_{M'_J} a_{M_J} \rangle \times \int_0^{\Delta t} dt \exp[-(\gamma + i\omega_{FF'})t] \,, \quad (28)$$

where

$$U(qq' M_J M'_J FF' J J_0) = [(2F+1)(2F'+1)(2J+1)/(2I+1)]\,(-)^{J_0+q-M_J} \times \sum_{\chi\nu} (2\chi+1)(-1)^{-\chi} \begin{Bmatrix} J & J & \chi \\ F' & F & I \end{Bmatrix}^2 \begin{Bmatrix} J & J & \chi \\ 1 & 1 & J_0 \end{Bmatrix} \begin{pmatrix} J & J & \chi \\ -M'_J & M_J & \nu \end{pmatrix} \begin{pmatrix} 1 & 1 & \chi \\ -q & q' & \nu \end{pmatrix} \,. \quad (29)$$

2. *Nonradiating Atom Violating LS Coupling*

Our assumptions leading to Eqs. (15) and (21) do not hold when the target atom or any atom formed in the collision violates the *LS* coupling rules, even though the radiating atom obeys them. For example, the Ly-α radiation formed by charge transfer of protons on Xe originates from the $2p$ state of the hydrogen atom, which obeys *LS* coupling, but the states of Xe and Xe^+ do not. In this case total electronic spin is not a good quantum number of the system and Eq. (12) no longer holds.

Three different situations may occur which are not described by Eq. (12): (a) The T operator in Eq. (8) may depend explicitly upon spin; (b) the states i and f may not obey *LS* coupling rules; or (c) the state vectors for the states i and f may approximately obey *LS* coupling, but some of the substates of their multiplets may not be energetically accessible. In all three cases the amplitudes $a(JM_J)$, where JM_J refer to the state of the radiating atom, can still be related to amplitudes $a(LM_LSM_S)$ by a Clebsch-Gordan transformation. Now, however, Eq. (9) no longer holds and amplitudes referring to different M_S states can interfere. Because of this interference, no reduction in the number of unknown parameters ensues from the transformation to the LM_LSM_S representation. Thus we use the JM_J representation for amplitudes describing the formation of the radiating atom as well. Because the radiative decay does not change the spin of the excited atom, however, we will use the *LS* representation to evaluate the dipole matrix element. Our expression for $A_{qq'}$ in this case differs from Eq. (29) only in that account is taken of interference between amplitudes referring to different J levels, since the different J levels may only be separated by a spacing of the same order as their widths. All manipulations made in deducing Eq. (17) can be repeated for this case and one finds

$$A_{qq'} = \sum_{JJ'FF'M_JM'_J} U(qq' M_J M'_J J J' FF' L L_0) \langle a_{J'M'_J} a_{JM_J} \rangle \int_0^{\Delta t} dt \exp[-(\gamma + i\omega_{JFJ'F'})t] \,, \quad (30)$$

where

$$U(qq' M_J M'_J J J' FF' L L_0) = \{[(2J+1)(2J'+1)]^{1/2} (2F+1)(2F'+1)(2L+1)[1/(2I+1)(2S+1)]\}\,(-1)^{S+L_0+q-M_J}$$

$$\times \sum_{\chi\nu} (2\chi+1) \begin{Bmatrix} J & J' & \chi \\ F' & F & I \end{Bmatrix}^2 \begin{Bmatrix} J & J' & \chi \\ L & L & S \end{Bmatrix} \begin{Bmatrix} L & L & \chi \\ 1 & 1 & L_0 \end{Bmatrix} \begin{pmatrix} J' & J & \chi \\ -M_{J'} & M_J & \nu \end{pmatrix} \begin{pmatrix} 1 & 1 & \chi \\ -q & q' & -\nu \end{pmatrix} . \quad (31)$$

To apply this equation to a noncoincidence measurement of Ly-α radiation produced in charge exchange, $d\Omega$ in Eq. (15) is integrated over, and only the quantities A_{00} and A_{11} enter into the expressions for the number of photons. These expressions, even though they apply to Ly-α radiation, now differ from Percival and Seaton's.[8] They differ because electronic spin is no longer a good quantum number of the target-projectile system, even though it is a good quantum number for the states of hydrogen atom alone.

III. SEMICLASSICAL MODEL OF ANGULAR DISTRIBUTION

The theory of the preceding section relates the angular distribution of the coincidences to the parameters of the initial-state wave function. The connection between the experimentally observed quantity, the angular distribution, and the initial-state wave function is somewhat remote, involving many mathematical manipulations which are difficult to interpret physically. To aid our understanding of the theory, we consider an alternative approach, which proceeds by constructing a classical source with the angular distribution given by Eq. (15). This approach was also used by Percival and Seaton.[8,14] Their source consisted of one oscillator oriented along the beam axis and two equal strength oscillators oriented perpendicular to each other and to the beam axis. The three oscillators emitted incoherently thus maintaining cylindrical symmetry about the beam axis. In our case the source is more complicated and will in general be made up of oscillators radiating coherently [to represent the sums in Eqs. (3) and (12) performed before squaring], and oscillators radiating incoherently (to represent the sums performed after squaring). It is clear that the equivalent source for the most general case is rather complicated, and little can be gained by constructing it. However, the presence of oscillators radiating coherently represents the new feature of the source with the angular distribution of Eq. (15). This feature can be illustrated, and its significance for future investigations discussed, for the special cases of Sec. II.

Consider first the $^1P - {}^1S$ transitions in He excited by electron or proton impact, for example. The collision prepares the atom in the state

$$\psi = a_0\psi_0 + a_1\psi_1 + a_{-1}\psi_{-1} . \quad (32)$$

ψ is invariant to reflections in the plane of scattering, and therefore

$$a_1 = -a_{-1} , \quad (33)$$

with the Condon-Shortley phase convention.

Thus

$$\psi = a_0\psi_0 + a_1(\psi_1 - \psi_{-1}) = a_0\psi_z - a_1\sqrt{2}\,\psi_x , \quad (34)$$

where the z and x subscripts denote the angular part of the wave functions. Now we can write ψ in terms of wave functions referred to a new z axis, called here the z' axis, oriented at an angle α to the old z axis and lying in the plane of scattering. Then ψ becomes

$$\psi = [a_0\cos\alpha + a_1\sqrt{2}\,\sin\alpha\,]\psi_{z'} + [a_0\sin\alpha - a_1\sqrt{2}\cos\alpha]\psi_{x'} = a_{z'}\psi_{z'} + a_{x'}\psi_{x'} . \quad (35)$$

Now α can always be chosen so that $a_{z'}$ and $a_{x'}$ differ in phase by 90°:

$$\tan 2\alpha = \frac{2\sqrt{2}\,\mathrm{Re}(a_0 a_1^*)}{\sigma_0 - 2\sigma_1} . \quad (36)$$

With this choice of α the angular distribution of the radiation is proportional to

$$|\,(0\,|\,\hat{\epsilon}\cdot\vec{x}\,|\,\psi)\,|^2 = (\hat{\epsilon}\cdot\vec{d}_1)^2 + (\hat{\epsilon}\cdot\vec{d}_2)^2 ,$$

where

$$\vec{d}_1 = (0\,|\,x\,|\,\psi_x)\,|\,a_{x'}\,|\,\hat{x}' ,$$

$$\vec{d}_2 = (0\,|\,z\,|\,\psi_z)\,|\,a_{z'}\,|\,\hat{z}' .$$

This distribution is identical to the average over one period of the radiation from two classical oscillators $\vec{d}_1$ and $\vec{d}_2$, oscillating 90° out of phase, oriented perpendicular to each and lying in the scattering plane as shown in Fig. 3(a).

The length of the two oscillators is proportional to the magnitudes of $a_{z'}$ and $a_{x'}$. As the dipoles oscillate they trace out an ellipse. The radiation emitted by the oscillators may be viewed perpendicular to the scattering plane with a polarizer oriented at an angle β' with respect to the major axis of the ellipse (or at an angle $\beta = \beta' + \alpha$ to the beam axis). The intensity observed is proportional to

$$I \propto |\,a_{z'}\,|^2\cos^2\beta' + |\,a_x\,|^2\sin^2\beta' . \quad (37)$$

A schematic polar plot illustrating the variation of I with β' appears in Fig. 3(b). From this figure we easily read off $|\,a_{z'}\,|$ and $|\,a_{x'}\,|$. Since we know that $a_{x'}$ and $a_{z'}$ differ in phase by 90°, we have determined ψ up to an over-all phase factor (actually one does not know whether the dipole vector rotates clockwise or counterclockwise; this requires a measurement of the circular polarization).

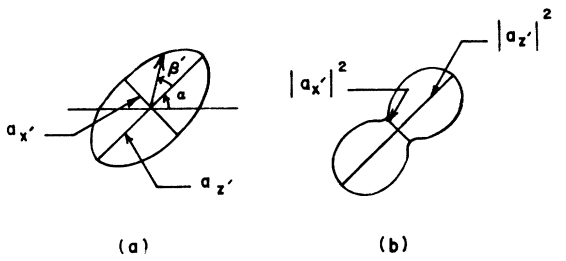

FIG. 3. Polarization of light emitted perpendicular to the scattering plane for $^1P-{}^1S$ transitions in He. (a) gives the measured distribution and (b) shows the equivalent classical source.

This construction also shows why the radiation from $^1P \rightarrow {}^1S$ transitions viewed perpendicular to the scattering plane is proportional to the total (for a given scattering angle) cross section. Effectively one sees the full length of both oscillators. At any other angle we see a projection of the oscillators which distorts the length of one compared to the other.

When the levels are split by fine or hyperfine structure, Eq. (35) still represents the wave function of the excited atom at $t=0$. However, since $\psi_{z'}$ and $\psi_{x'}$ are not eigenstates of the target, at later times they evolve into spin dependent linear combinations of $\psi_{x'}$, $\psi_{y'}$, and $\psi_{z'}$. This evolution tends to smear out the angular distribution, however the dipole vectors at $t=0$ still serve to characterize the collisional excitation process.

Our classical construction suggests that the experimental data for $P \rightarrow S$ transitions may be graphically presented in terms of the two dipole vectors just discussed. The vectors are directly measured only for $P \rightarrow S$ transitions with no fine- or hyperfine-structure depolarization, as for the $^1P \rightarrow {}^1S$ transitions in He[4].

When fine structure or hyperfine structure is present the amplitude a_0 and a_1 can be extracted from Eq. (15) provided Eq. (22) holds. Then the dipole vectors may be constructed using Eqs. (35) and (36). A determination of these vectors over a wide range of energies will provide substantially new information on atomic collision processes, in particular, it will provide information on how excitation processes depart from predictions of the Born theory. In the Born approximation, the ellipse traced out by the dipole vectors degenerates into a straight line parallel to the momentum-transfer vector. Departures are manifested by (a) a rotation of the line from an orientation along the momentum transfer axis, (b) a broadening of the ellipse, (c) a contraction or expansion of the degenerate ellipse away from the magnitude predicted by the Born theory. Experimental determination of the relative importance of these three types of departures will provide substantially new information on the excitation process.

As a second example of the usefulness of the data provided by coincidence experiments, consider excitation or charge transfer in heavy-ion collisions in the adiabatic region. Here the change of the projection of the electronic angular momentum along the internuclear axis serves to classify the excitation mechanism. Direct excitations, which occur because of the translational kinetic energy perturbation to the temporarily formed molecular system, obey the $\Delta\lambda = 0$ rule, while those which occur because of the rotational coupling obey the $\Delta\lambda = \pm 1$ rule. Here λ is the projection of the electronic angular momentum on the internuclear axis. As long as the relation (33) holds, the $\Delta\lambda = 0$ excitations will correspond to a dipole vector oriented along the direction of the outgoing particle while $\Delta\lambda = \pm 1$ excitations correspond to the dipole vector oriented perpendicular to direction of the outgoing particle. Coincidence techniques thus make possible the experimental differentiation of these two mechanisms.

IV. TIME INTEGRATION

As we have suggested in the Introduction, the theory of Sec. II may be applied to noncoincidence experiments as well as coincidence experiments. One only need integrate Eq. (16) over the solid angle of the particle detector. The resulting equations, however, do not reduce to the Percival and Seaton theory unless one further assumes that the emitting atom remains in view of the photon detector for a time long compared to the mean life of the excited atom. This condition is not always met in charge exchange measurements and corrections for the finite lifetime of the atom must be made. Corrections are usually made by solving the classical rate equations[9] for the number of excited atoms. This approach is appropriate as long as the experiment actually measures a quantity proportional to the number of excited atoms. Such measurements may be accomplished by measuring the light intensity integrated over all angles and summed over both polarizations; however, one often wishes to measure the polarization of the radiation as well as its integrated intensity. This requires a measurement of a light intensity which is not proportional to the number of atoms in the excited state. The instantaneous intensity could be obtained here using rate equations for the density matrix describing the initial-state population.[15] Alternatively, one may simply integrate Eq. (16) over time in a manner appropriate to the particular experimental geometry. Since this latter approach is more direct, and since the classical rate equation approach has often been used without any discussion of the applicability of the procedure, we

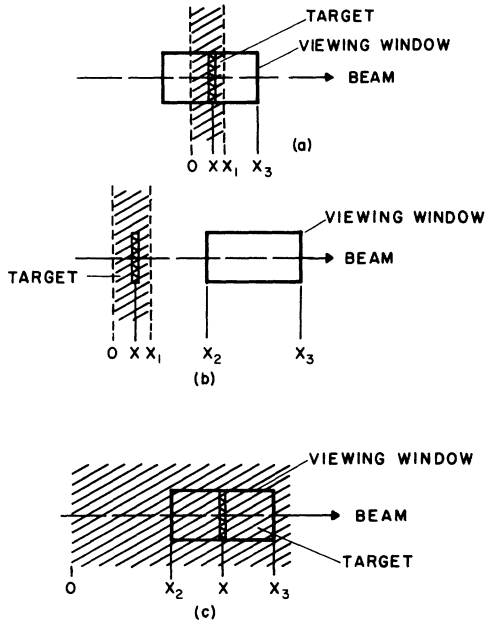

FIG. 4. Schematic collision geometries requiring different time integrations. (a) Crossed beam, (b) decay curve measurement, and (c) flooded collision chamber.

will discuss the time integrations for the three commonly encountered geometries shown in Fig. 4.

The schematic diagrams in Fig. 4 contain three parts: (a) the target gas configuration, (b) the proton beam, and (c) the schematic viewing window. The length of the viewing window is the parameter of most importance here. This length is represented geometrically, but its effective length is not always the geometrical length. If v is the velocity of the incoming proton and if t_d is the delay time between the detection of a photon and the detection of a particle, then only photons emitted when the atom is at a distance greater than $(t_d - \Delta t/2)v$ but less than $(t_d + \Delta t/2)$ from the particle detector are counted as real coincidences. Here Δt is the resolution time. Thus $\Delta d = v\Delta t$ essentially measures the length of the viewing window as long as Δd is less than the geometrical length viewed by the photon detector. With this interpretation of the schematic diagrams, we consider the three experimental configurations.

(a) Crossed beam. Here the proton crosses a beam of neutral particles and picks up an electron in an excited state at some point x in the gas beam. The number of atoms so formed is proportional to $n_A(x)$ the number of atoms in a thin volume element of thickness dx whose sides are perpendicular to the proton beam. Taking the zero of time when the atom is at the leftmost edge of the gas target, the probability that the excited atom formed at x will decay in a time dt is proportional to

$$e^{-\gamma(t-x/v)}\,dt\,, \quad t > x/v\,. \tag{38}$$

A typical time-dependent factor in Eq. (16) also contains $e^{i\Omega t}$, where Ω is short for $\omega_{JFJ'F'}$. To obtain the number of photons detected we must integrate the time-dependent factor over x and t, weighted by $n_A(x)$. The factor

$$n_A \int_0^{\Delta t} e^{-\Gamma t}$$

in Eq. (16) is then replaced by

$$\int_0^{x_1} dx\, n_A(x) \int_{x/v}^{x_3/v} dt\, e^{-\Gamma(t-x/v)}\,, \tag{39}$$

where $\Gamma = \gamma + i\Omega$.

(b) Decay-curve measurements. In this case all excited atoms are formed outside of the viewing window. The integrals are identical to Eq. (39) except that the lower limit x/v is replaced by x_2/v.

(c) Flooded collision chamber. Here some atoms are formed prior to entering the viewing region, as in case (b), and some are formed in the viewing region, as in case (a). The number of photons counted is obtained by adding the two contributions. The combined integral is

$$\int_{x_2}^{x_3} dx\, n_A(x) \int_{x/v}^{x_3/v} dt\, e^{-\Gamma(t-x/v)} + \int_0^{x_2} dx\, n_A(x) \int_{x_2/v}^{x_3/v} dt\, e^{-\Gamma(t-x/v)}\,. \tag{40}$$

To connect these expressions with those obtained by a rate equation approach, we will evaluate the integrals for the cases considered by Hughes, *et al.*[9] [case (b)] and by Jaecks[9] [case (c)]. In case (b) considered by Hughes *et al.*,[9] the condition $(x_3 - x_2)/v \ll 1/\gamma$ holds, so the integral over t was not performed. Then setting $n_A(x) = \text{const}$ and replacing t by x_2/v we get for the integral over x

$$-e^{-\Gamma x_2/v}(1 - e^{\Gamma x_1/v}) = e^{-\Gamma(x_2-x_1)/v}(1 - e^{-\Gamma x_1/v})\,. \tag{41}$$

When $\Gamma = \gamma$, this is precisely the result obtained by Hughes *et al.*[9] However, since Eq. (16) contains terms with $\Omega \neq 0$, the result obtained from a rate equation approach can only be applied when the light intensity being measured is proportional to the intensity integrated over all directions and summed over polarizations, or when corrections introduced by the nonvanishing of Ω are negligible. Such corrections are small when the ratio γ/Ω is small compared to unity, since then the coefficients of the oscillatory terms are small compared to those of the nonoscillatory terms. The corrections are also small if γ/Ω is much larger than unity, since then the atom decays before the oscillations produce a noticeable effect. Between these two limits the corrections must be evaluated for each geometrical arrangement. Use of a rate equation approach by Hughes *et al.* is quite correct, however, since they measured the radiation

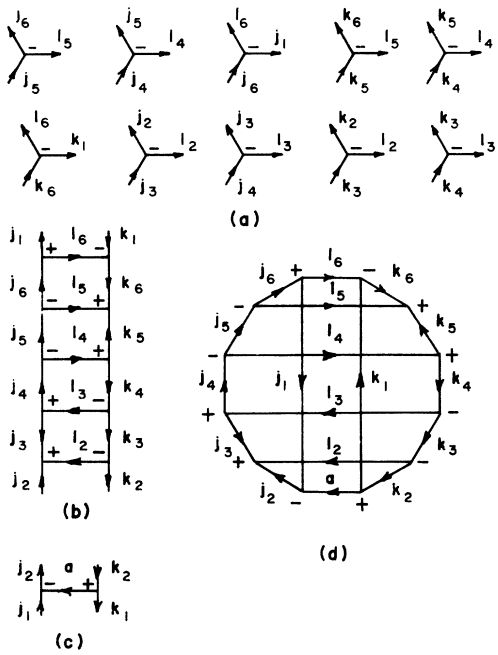

FIG. 5. Evaluation of a sum of Clebsch-Gordan coefficients by diagrams. The ten diagrams in Fig. 5(a) represent the products of ten Clebsch-Gordan coefficients. The diagrams are joined to form Fig. 5(b), which is contracted with Fig. 5(c) to obtain Fig. 5(d).

from an S state, which is unpolarized and isotropic. For such radiation, terms containing $\Omega \neq 0$ do not enter into the expression for the angular distribution.

In the expression considered by Jaecks[9] the condition $(x_3 - x_2)/v \ll 1/\gamma$ also applies and the integration over t in Eq. (40) simply replaces t by x_2/v and multiplies the integrand by the factor $(x_3 - x_2)/v$. The first term of Eq. (40) is second order in $(x_3 - x_2)/v$ and is negligible compared to the second term, which becomes, upon taking $n_A(x) = \text{const}$,

$$(1 - e^{-\Gamma x_2/v})/\Gamma \ . \tag{42}$$

When $\Gamma = \gamma$ this equals the result obtained from the rate equation theory. When $x \to \infty$, we get just $1/\Gamma$ which is the result obtained by Percival and Seaton.[8] Note that $x \to \infty$, or more precisely, $x_2/v \gg \gamma$, is realized by allowing the proton beam to pass through a long gas-filled collision chamber. Thus Percival and Seaton's theory applies here even though a particular atom remains in view of the photon detector for only a short time. Since Gaily *et al.*[9] actually ensured that $x_2/v \gg \gamma$, their use of Percival and Seaton's theory is fully justified.

APPENDIX: EVALUATION OF SUM OVER CLEBSCH-GORDAN COEFFICIENTS

We evaluate the sum

$$\begin{aligned} C = \sum_B\ & (j_6 m_6 l_5 n_5 \mid j_6 l_5 j_5 m_5)(j_5 m_5 l_4 n_4 \mid j_5 l_4 j_4 m_4) \\ & \times (l_6 n_6 j_1 m_1 \mid l_6 j_1 j_6 m_6)(k_6 r_6 l_5 n_5 \mid k_6 l_5 k_5 r_5) \\ & \times (k_5 r_5 l_4 n_4 \mid k_5 l_4 k_4 r_4)(l_6 n_6 k_1 r_1 \mid l_6 k_1 k_6 r_6) \\ & \times (j_2 m_2 l_2 n_2 \mid j_2 l_2 j_3 m_3)(j_3 m_3 l_3 n_3 \mid j_3 l_3 j_4 m_4) \\ & \times (k_2 r_2 l_2 n_2 \mid k_2 l_2 k_3 r_3)(k_3 r_3 l_3 n_3 \mid k_3 l_3 k_4 r_4) \ , \end{aligned} \tag{A1}$$

where B stands for the set $m_3 m_4 m_5 m_6 n_2 n_3 n_4 n_5 n_6 r_3 r_4 r_5 r_6$, using the diagrammatic technique of Yutsis.[16] We first write the Clebsch-Gordan coefficients in terms of the Wigner $3-j$ symbols[13]

$$(j_1 m_1 j_2 m_2 \mid j_1 j_2 j_3 m_3) = (-)^{j_1 - j_2 + j_3} (j_3)^{1/2} (-)^{j_3 - m_3} \times \begin{pmatrix} j_1 & j_2 & j_3 \\ m_1 & m_2 & -m_3 \end{pmatrix} \ , \tag{A2}$$

where (j_3) equals $(2j_3 + 1)$. This converts the sum over Clebsch-Gordan coefficients into a sum over $3-j$ symbols:

$$\begin{aligned} C = A(-)^{R_1} \sum_B{}' & \begin{pmatrix} j_6 & l_5 & j_5 \\ m_6 & n_5 & -m_5 \end{pmatrix} \begin{pmatrix} j_5 & l_4 & j_4 \\ m_5 & n_4 & -m_4 \end{pmatrix} \\ & \times \begin{pmatrix} l_6 & j_1 & j_6 \\ n_6 & m_1 & -m_6 \end{pmatrix} \begin{pmatrix} k_6 & l_5 & k_5 \\ r_6 & n_5 & -r_5 \end{pmatrix} \begin{pmatrix} k_5 & l_4 & k_4 \\ r_5 & n_4 & -r_4 \end{pmatrix} \begin{pmatrix} l_6 & k_1 & k_6 \\ n_6 & r_1 & -r_6 \end{pmatrix} \\ & \times \begin{pmatrix} j_2 & l_2 & j_3 \\ m_2 & n_2 & -m_3 \end{pmatrix} \begin{pmatrix} j_3 & l_3 & j_4 \\ m_3 & n_3 & -m_4 \end{pmatrix} \begin{pmatrix} k_2 & l_2 & k_3 \\ r_2 & n_2 & -r_3 \end{pmatrix} \begin{pmatrix} k_3 & l_3 & k_4 \\ r_3 & n_3 & -r_4 \end{pmatrix} , \end{aligned} \tag{A3}$$

where

$$A = [(j_3)(j_4)^2 (j_5)(j_6)(k_3)(k_4)^2 (k_5)(k_6)]^{1/2} \tag{A4}$$

and

$$\begin{aligned} R_1 = & -j_1 + j_2 + 2j_3 - j_4 + 2j_5 + 2j_6 - k_1 + k_2 + 2k_3 - k_4 \\ & + 2k_5 + 2k_6 + l_2 + l_3 + l_4 + l_5 + l_6 - r_2 - m_1 \ . \end{aligned} \tag{A5}$$

The prime on the summation sign indicates that for each magnetic quantum number m summed over, there corresponds the factor $(-)^{j-m}$.

The diagrams corresponding to the sum over $3-j$ symbols in Eq. (A3) are shown in Fig. 5(a). These diagrams are joined according to Yutsis's[16] rules to form Fig. 5(b). Interchanges performed to relate Figs. 5(a) and 5(b) show that the coefficient represented by Fig. 5(a) equals the coefficient represented by Fig. 5(b) multiplied by the factor

$$(-)^{j_2 + j_4 + k_1 + k_4 + 2k_6 + l_2 + l_3 + l_4 + l_5 + l_6} \ . \tag{A6}$$

The diagram in Fig. 5(b) is contracted with the diagram in Fig. 5(c) to form the diagram in Fig. 5(d), which is recognized as an $18-j$ symbol of the second kind multiplied by the factor

$$(-)^{j_1 + j_4 + 2(j_3 + j_5 + j_6) + k_1 - k_4 + 2(k_2 + k_3 + k_5)} \ . \tag{A7}$$

According to Yutsis's rules, the sum represented by Fig. 5(a) is then given, to within a sign factor, by the $18-j$ coefficient multiplied by the two Clebsch-Gordan coefficients represented in Fig.

5(c) and summed over a. Combining this result with the factors Eqs. (A4), (A3), (A6), and (A7), we have

$$C = A(-)^{R_2} \sum_{a\mu} (a)(-)^{a-\mu} \begin{bmatrix} j_1 & j_2 & j_3 & j_4 & j_5 & j_6 \\ a & l_2 & l_3 & l_4 & l_5 & l_6 \\ k_1 & k_2 & k_3 & k_4 & k_5 & k_6 \end{bmatrix} \times \begin{pmatrix} j_1 & j_2 & a \\ -m_1 & m_2 & -\mu \end{pmatrix} \begin{pmatrix} a & k_1 & k_2 \\ \mu & r_1 & -r_2 \end{pmatrix}, \quad \text{(A8)}$$

where [ ] represents an $18-j$ symbol of the second kind and R_2 is given by

$$R_2 = 2j_2 + j_4 - k_1 + k_2 - k_4 - r_2 - m_1 . \quad \text{(A9)}$$

In Eq. (A9) we have used relations such as

$$2(j_5 + j_6 + l_5) = \text{even}$$

to equate some sign factors to unity.

The $18-j$ coefficient can be written directly in terms of Racah coefficients[16]

$$\begin{bmatrix} j_1 & j_2 & j_3 & j_4 & j_5 & j_6 \\ a & l_2 & l_3 & l_4 & l_5 & l_6 \\ k_1 & k_2 & k_3 & k_4 & k_5 & k_6 \end{bmatrix} = (-)^{R_3} \sum_{\chi} (\chi)(-)^{2\chi} \begin{Bmatrix} j_1 & k_1 & \chi \\ k_2 & j_2 & a \end{Bmatrix} \times \begin{Bmatrix} j_2 & k_2 & \chi \\ k_3 & j_3 & l_2 \end{Bmatrix} \begin{Bmatrix} j_3 & k_3 & \chi \\ k_4 & j_4 & l_3 \end{Bmatrix} \begin{Bmatrix} j_4 & k_4 & \chi \\ k_5 & j_5 & l_4 \end{Bmatrix} \begin{Bmatrix} j_5 & k_5 & \chi \\ k_6 & j_6 & l_5 \end{Bmatrix} \times \begin{Bmatrix} j_6 & k_6 & \chi \\ k_1 & j_1 & l_6 \end{Bmatrix}, \quad \text{(A10)}$$

where $R_3 = \sum_i (j_i + k_i + 1_i)$, with l_1 set equal to a.

Substituting Eq. (A10) in Eq. (A8), we see that the sum over a and μ can be carried out since[13]

$$\sum_{a\mu} (-)^{2a-\mu} \begin{Bmatrix} j_1 & k_1 & \chi \\ k_2 & j_2 & a \end{Bmatrix} \begin{pmatrix} j_1 & j_2 & a \\ -m_1 & m_2 & -\mu \end{pmatrix} \begin{pmatrix} a & k_1 & k_2 \\ \mu & r_1 & -r_2 \end{pmatrix} = (-)^{k_2+k_1-3\chi-m_2+r_2+2m_1} \sum_{\nu} \begin{pmatrix} k_2 & j_2 & \chi \\ -r_2 & m_2 & \nu \end{pmatrix} \begin{pmatrix} j_1 & k_1 & \chi \\ -m_1 & r_1 & -\nu \end{pmatrix}. \quad \text{(A11)}$$

Substituting Eqs. (A10) and (A11) into Eq. (A8) then gives our final result

$$C = A(-)^{R} \sum_{\chi\nu} (\chi)(-)^{-\chi} \begin{Bmatrix} j_2 & k_2 & \chi \\ k_3 & j_3 & l_2 \end{Bmatrix} \begin{Bmatrix} j_3 & k_3 & \chi \\ k_4 & j_4 & l_3 \end{Bmatrix} \begin{Bmatrix} j_4 & k_4 & \chi \\ k_5 & j_5 & l_4 \end{Bmatrix} \times \begin{Bmatrix} j_5 & k_5 & \chi \\ k_6 & j_6 & l_5 \end{Bmatrix} \begin{Bmatrix} j_6 & k_6 & \chi \\ k_1 & j_1 & l_6 \end{Bmatrix} \begin{pmatrix} k_2 & j_2 & \chi \\ -r_2 & m_2 & \nu \end{pmatrix} \begin{pmatrix} j_1 & k_1 & \chi \\ -m_1 & r_1 & -\nu \end{pmatrix}, \quad \text{(A12)}$$

where

$$R = R_3 - a + 2j_2 + j_4 + 2k_2 - k_4 + m_1 - m_2 .$$

*Supported in part by a grant from the National Science Foundation.

[1]H. Ehrhardt, M. Schulz, T. Tekaat, and K. Willmann, Phys. Rev. Letters 22, 89 (1969).

[2]J. R. Sheridan, Rev. Sci. Instr. 40, 358 (1969).

[3]V. Weisskopf and E. Wigner, Z. Physik 65, 18 (1930).

[4]D. H. Jaecks, D. H. Crandall, and R. H. McKnight, Phys. Rev. Letters 25, 491 (1970).

[5]L. C. Biedenharn, in *Nuclear Spectroscopy, Part B*, edited by Fay Ajzenberg-Selove (Academic, New York, 1960).

[6]K. Schilling, P. Seyboth, and G. Wolf, Nucl. Phys. B15, 397 (1970).

[7]J. Macek, Phys. Rev. Letters 23, 1 (1969); Phys. Rev. A 1, 618 (1970).

[8]I. Percival and M. Seaton, Phil. Trans. Roy. Soc. London A251, 113 (1958).

[9]R. H. Hughes, H. R. Dawson, B. M. Doughty, D. B. Kay, and C. A. Stigers, Phys. Rev. 146, 53 (1966); D. Jaecks, Ph.D. thesis (University of Washington, 1964) (unpublished); T. D. Gaily, D. H. Jaecks, and R. Geballe, Phys. Rev. 167, 81 (1968).

[10]P. Franken, Phys. Rev. 121, 508 (1961).

[11]F. H. Read and R. E. Imhof, Chem. Phys. Letters 13, 652 (1969).

[12]H. J. Andra, Phys. Rev. Letters 25, 325 (1970).

[13]A. Edmunds, *Angular Momentum in Quantum Mechanics* (Princeton U. P., Princeton, New Jersey, 1957).

[14]J. A. Smit, Physica 2, 104 (1935).

[15]T. Hadishi, Phys. Rev. 162, 16 (1967).

[16]A. P. Yutsis, I. B. Levinson, and V. V. Vanagas, *Theory of Angular Momentum* (National Science Foundation, Washington, D. C., 1960).